This is the author-version of an article published as:

Frost, Ray and Weier, Matt and Martens, Wayde and Cejka, Jiri (2006) Molecular structure of the uranyl silicates –A Raman spectroscopic study. *Journal of Raman Spectroscopy* 37(4):pp. 538-551.

Molecular structure of the uranyl silicates –A Raman spectroscopic study

Ray L. Frost[•] [a], Jiří Čejka [b], Matt L Weier [a] and Wayde Martens [a]

Inorganic Materials Research Program, School of Physical and Chemical Sciences, Queensland University of Technology, GPO Box 2434, Brisbane Queensland 4001, Australia.

[b] National Museum, Václavské náměstí 68, CZ-115 79 Praha 1, Czech Republic.

Abstract

Raman spectroscopy has been used to study the molecular structure of a series of selected uranyl silicate minerals including uranophane, sklodowskite, cuprosklodowskite, boltwoodite and kasolite. Raman spectra clearly show well resolved bands in the 750 to 800 cm^{-1} region and in the 950 to 1000 cm^{-1} region assigned to the ν_1 modes of the $(UO_2)^{2+}$ units and to the $(SiO_4)^{4-}$ tetrahedra. Sets of Raman bands in the 200 to 300 cm^{-1} region are assigned to ν_2 δ $(UO_2)^{2+}$ and UO ligand vibrations. Multiple bands indicate the non-equivalence of the UO bonds and the lifting of the degeneracy of ν_2 δ $(UO_2)^{2+}$ vibrations. The $(SiO_4)^{4-}$ tetrahedral are characterized by bands in the 470 to 550 cm^{-1} and in the 390 to 420 cm^{-1} region. These bands are attributed to the ν_4 and ν_2 $(SiO_4)^{4-}$ bending modes. The minerals show characteristic OH stretching bands in the 2900 to 3500 cm^{-1} and 3600 to 3700 cm^{-1} region ascribed to water stretching and SiOH stretching vibrations. The high wavenumber position of the δH_2O bands indicate strong hydrogen bonding of water in these uranyl silicates. Bands in the 1400 to 1550 cm^{-1} region are attributed to δSiOH modes. The Raman spectroscopy of uranyl silicate minerals enabled separation of the bands attributed to distinct vibrational units. This enabled definitive assignment of the bands. The spectra are analysed in terms of the molecular structure of the minerals.

Key words: uranyl silicate minerals, uranophane, sklodowskite, cuprosklodowskite, kasolite, boltwoodite, infrared and Raman spectroscopy

[•] Author to whom correspondence should be addressed (r.frost@qut.edu.au)

Introduction

According to Burns (2001), uranyl silicates are common constituents of the oxidized portions of uranium deposits and typically form as a results of their alteration of uraninite [1]. They are important for understanding the genesis of uranium deposits, as well as fluid-rock interaction during the hydration-oxidation weathering of uranium deposits or the mine and mill tailings that result from resource utilization. Uranyl silicates are also significant to the disposal of nuclear waste.

Uranyl silicates are likely to be abundant in a geological repository for nuclear waste under moist oxidizing conditions, owing to the alteration of spent nuclear fuel and borosilicate waste glass. An understanding of the structures of uranyl silicates may be a key to understanding the long-term performance of a geological repository for nuclear waste [2,3]. It is likely that uranyl compounds forming due to alteration of nuclear waste incorporate radionuclides into their crystal structures.

Nine uranyl silicate minerals (uranophane, sklodowskite, cuprosklodowskite, boltwoodite, sodium boltwoodite, kasolite, oursinite and swamboite) have been classified as members of the uranophane group on the basis of the UO_2^{2+}/SiO_2 molar ratio being 1:1 and a similar uranophane anion sheet topology [4-7]. β-uranophane is a polymorph of uranophane (α-uranophane), and the details of their structural connectivities differ substantially [6,8]. Soddyite is characterized by the UO_2^{2+}/SiO_2 molar ratio 2:1 and framework crystal structure [6,9]. The crystal structure of $Na_2(UO_2)_2SiO_4F_2$ is structurally related to soddyite [10]. The molar ratio UO_2^{2+}/SiO_2 2:5 was found in the crystal structures of weeksite [2], haiweeite [1], coutinhoite [11]

and probably also in some not approved uranyl silicate minerals from Russia [12,13]. Some synthetic framework uranyl silicates were also described [14,15]

Čejka reviewed all available data on infrared spectra of uranyl silicate minerals and their synthetic analogues (Čejka 1999 and many references therein) [16]. Biwer et al. shortly described the only available Raman spectra of uranophane, sodium boltwoodite, weeksite and soddyite without any detailed interpretation [17]. Plesko et al. presented infrared vibrational characterization and synthesis of a family of hydrous alkali uranyl silicates and hydrous uranyl silicate minerals, however, their interpretation may be questionable [18]. Chernorukov's research group prepared monovalent and divalent uranyl silicates and presented their properties inclusive interpretation of the infrared spectra [19-28]. As proved by Čejka (1999), some infrared spectra uranyl silicate minerals including their assignment have been published but only very limited number of Raman spectra of these minerals without any detailed attribution are available. Some discrepancies in the IR spectra of uranyl silicate minerals published by various authors may be observed caused probably by ill-defined minerals, different IR spectrophotometers used for the measurements, and incorrect crystallochemical formulas used for the interpretation and inadequate or inappropriate treatment of the spectra. In this paper, the Raman and IR spectra of uranyl silicate minerals are interpreted respecting the newest single crystal structures of individual minerals, accepted and approved chemical formulas, and crystallochemical application of uranyl anion sheet topology established by Burns [6,7,29,30].

Akhmanova et al. (1963) proved the position of silanol, SiOH, vibrations in $(SiO_3OH)^{3-}$ ions in the IR spectrum of minerals [31]. This was supported by Plyusnina

(1977) [32] and for the uranyl silicate minerals by Gevorkyan [33,34], Čejka and Urbanec (1990), and Čejka (1999) [16,35]. However the positioning of a SiOH band at 3200 cm-1 is contrary to the expected position of 3700 cm-1 or higher. Bands in this position are found for zeolites and clay minerals. Vochten et al. (1997) confirmed this observation in the IR spectrum of natural and synthetic boltwoodite and synthetic uranophane and sklodowskite [36]. On this basis, Burns inferred the presence of SiOH in the single crystal structure of boltwoodite [6]. Nyfeler and Armbuster (1998) discussed silanol groups in minerals and inorganic compounds [37]. Chernorukov et al. (see above for details) also assigned some bands in the IR spectra of synthetic uranyl silicates to silanol groups.

In this paper, Raman and infrared spectra of uranophane, sklodowskite, cuprosklodowskite, kasolite and boltwoodite are reported. The minerals soddyite, weeksite, and haiweeite are studied in a separate paper. As a part of our on-going research into the use of vibrational spectroscopy in particular Raman spectroscopy to assist in the elucidation of the structures of minerals especially secondary minerals, we report the Raman and infrared spectra of some uranyl silicate minerals. These spectra are related to the recently known mineral structures.

Experimental

Minerals

The minerals used in this study and their origin are shown in Table 1. The minerals, where possible, were checked for phase purity by powder X-ray diffraction

and for chemical composition by Energy dispersive X-ray analysis. A significant number of minerals were collected and analysed but only those of the highest purity were used in this study.

Raman microprobe spectroscopy

The crystals of the uranyl silicate mineral was placed and orientated on the stage of an Olympus BHSM microscope, equipped with 10x and 50x objectives and part of a Renishaw 1000 Raman microscope system, which also includes a monochromator, a filter system and a Charge Coupled Device (CCD). Raman spectra were excited by a HeNe laser (633 nm) at a resolution of 2 cm^{-1} in the range between 100 and 4000 cm^{-1}. Repeated acquisition using the highest magnification was accumulated to improve the signal to noise ratio. Spectra were calibrated using the 520.5 cm^{-1} line of a silicon wafer. In order to ensure that the correct spectra are obtained, the incident excitation radiation was scrambled. Previous studies by the authors provide more details of the experimental technique. Spectra at liquid nitrogen temperature were obtained using a Linkam thermal stage (Scientific Instruments Ltd, Waterfield, Surrey, England). Details of the techniques which have been applied to the study of uranyl compounds have been published by the authors [38-44]. The band fitting protocols are provided in an appendix to this manuscript.

In Raman spectra, water is a very poor Raman scatterer; hence any bands attributable to water will be of low intensity or may not be observed. If the water is hydrogen bonded to an anion or coordinated to a cation, the symmetry of the water bonded unit may be lifted resulting in increased intensity of the bands. For example

the water bending mode normally observed as an intense band in the infrared spectra at 1630 cm^{-1} will not be observed in the Raman spectrum. If the water is bonded to for example a carbonate anion (as is the case for hydrotalcites) then a band of increased intensity at higher wavenumbers will be observed. In the Raman spectrum the antisymmetric stretching modes of water will be of low intensity but the symmetric stretching modes may be observed anywhere between 2900 and 3600 cm^{-1}. The more strongly hydrogen bonded water vibrational modes will be found at the lower wavenumber positions whilst the weakly hydrogen bonded water or non-hydrogen bonded water will be found at the higher wavenumber positions. If the mineral contains OH units the position of the OH symmetric stretching vibrations are normally found at positions higher than that for water.

Infrared Spectroscopy

Infrared spectra were obtained using a Nicolet Nexus 870 FTIR spectrometer with a smart endurance single bounce diamond ATR cell. Spectra over the 4000−525 cm^{-1} range were obtained by the co-addition of 64 scans with a resolution of 4 cm^{-1} and a mirror velocity of 0.6329 cm/s. Spectral manipulation such as baseline adjustment, smoothing and normalisation was performed using the GRAMS® software package (Galactic Industries Corporation, Salem, NH, USA).

It should be noted that previously published data were often reported as transmittance data, were not placed upon flat base lines and were not curve resolved. The spectra in this paper have all been converted to absorbance-like plots in the case of the infrared spectra, placed upon flat base lines, and curve resolved. The results reported in this paper may be different to the previously published results because of these factors.

Results and discussion

Raman spectroscopy has been used to study the molecular structure of a selected series of uranyl silicate minerals including uranophane, sklodowskite, cuprosklodowskite, boltwoodite and kasolite. The spectra may be divided into six spectral regions: (a) the OH stretching region between 2800 and 3600 cm^{-1} (b) the δH_2O bending region between 1595 and 1700 cm^{-1} (c) the $(UO_2)^{2+}$ stretching region between 790 and 900 cm^{-1} (d) the $(UO_2)^{2+}$ bending region between 200 and 340 cm^{-1} (e) the $(SiO_4)^{4-}$ stretching region between 900 and 1150 cm^{-1} and (f) the $(SiO_4)^{4-}$ bending region between 390 and 570 cm^{-1}.

The ideal linear uranyl group, $(UO_2)^{2+}$, with point group symmetry $D_{\infty h}$ has four normal vibrations, but only three fundamentals: the Raman active symmetric stretching vibration ν_1 (900-700 cm^{-1}), the doubly degenerate IR active bending vibration ν_2 (δ) (350-180 cm^{-1}), and the antisymmetric IR active stretching vibration ν_3 (1000-850 cm^{-1}). The decrease of uranyl group symmetry $D_{\infty h} \Rightarrow C_{\infty v}$ results in the IR activation of the ν_1 $(UO_2)^{2+}$, similarly, the change in symmetry $D_{\infty h} \Rightarrow C_{2v}$ adds the splitting of the doubly degenerate ν_2 $(UO_2)^{2+}$. The former activation may be caused by

the presence of nonequivalent bonds in uranyl, $(O\text{-}U\text{-}O)^{2+}$, the latter one in the linearity loss, i.e. $(O\text{-}U\text{-}O)^{2+}$ angle deformation. The ν_1 and ν_3 $(UO_2)^{2+}$ may also split in two or more components. This may be influenced especially because of the presence of symmetrically distinct uranyls in the unit cell and, splitting of degenerate vibrations, and also respecting the factor group analysis.

The ideal $(SiO_4)^{4-}$ tetrahedron with point group symmetry Td has nine normal vibrations characterized by four fundamental distinguishable modes of vibration: the Raman active symmetric stretching vibration ν_1 (A), (819 cm^{-1}), the Raman active doubly degenerate bending vibration ν_2 (E), (340 cm^{-1}), Raman and infrared active triply degenerate antisymmetric stretching vibration ν_3 (F_2), (956 cm^{-1}), and the Raman and infrared active triply degenerate bending vibration ν_4 (F_2), (527 cm^{-1}) [45]. The symmetry decrease from Td $\Rightarrow$ C_{3v}, which is the case of $(SiO_3OH)^{3-}$, results in IR activation of the ν_1 (A_1) and ν_2 (E), and splitting of the both ν_3 and ν_4 (both A_1 + E). The presence of one proton in the apex of the $(SiO_4)^{4-}$ tetrahedron, i. e. formation of $(SiO_3OH)^{3-}$, together with bonding of the remaining three oxygens in the uranyl silicate layers leads to lowering of the $(SiO_3OH)^{3-}$ site symmetry to C_s or C_1. This symmetry lowering is connected with IR and Raman activation of all vibrations, i.e. the ν_1 (A' or A), the ν_2 splits (A' + A'' or 2A), and further splitting of the ν_3 and ν_4 (2A' + A'' or 3A). The number of bands may be enhanced because of the presence of symmetrically distinct Si^{4+} in the crystal structure of some uranyl silicate minerals.

According to McMillan (1984), for the framework silicates and silicates with multilayer structures, their formation may be considered as polymerization of (SiO_4) tetrahedra by corner-sharing each oxygen with two (SiO_4) units [46]. This results in a

coupling of the ν_1 and ν_3 types of modes. The vibrations follow the frequency order ν_3 (Si-O-Si) > ν (Si-O^-) > ν_1 (Si-O-Si) > δ (Si-O-Si), δ (O-Si-O), where ν_3 (Si-O-Si) and ν_1 (Si-O-Si) refer to the antisymmetric and symmetric stretching modes of Si-O-Si bridges, ν (Si-O^-) represents the stretching (Si-O^-) bonds, δ (Si-O-Si) and δ (O-Si-O) refer to the Si-O-Si and O-Si-O bending modes [47,48]. According to Chernorukov et al. (2002), wavenumbers of bands attributed to silanols, Si-OH, are located near 3200 cm^{-1} (ν SiOH stretching mode), 1400 and 600 cm^{-1} (δ SiOH in-plane and out-of-plane bending mode, respectively) [27,28]. The most important for the interpretation may be the isolated band observed near 1400 cm^{-1} [16]. Similar conclusions were made for double $(Np^{6+}O_2)^{2+}$ and $(Pu^{6+}O_2)^{2+}$ potassium silicates $K[(NpO_2)(SiO_3OH)]. H_2O$ and $K[(PuO_2)(SiO_3OH)]. H_2O$ [49].

Water molecules possessing the point group C_{2v} are characterized by three fundamentals: ν OH stretching vibrations (ν_1 and ν_3 H_2O) (~3600 – 2900 cm^{-1}), and δ H_2O bending vibration (1700-1590 cm^{-1}). All vibrations are IR and Raman active. H_2O libration modes may occur in the range 1100-300 cm^{-1}. Hydroxyl ions, $(OH)^{-1}$, (point group symmetry $C_{\infty v}$) are usually indicated by sharp bands between 3700-3450 cm^{-1} but sometimes lower if any appreciable amount of hydrogen bonding is involved. The restricted rotational or libration motion of this ion occurs with a wavenumber usually in the 600-300 cm^{-1} range. The δ M-OH bending vibration may occur over a wide range below approximately 1500 cm^{-1}.

Uranophane group minerals

Uranyl stretching vibrations

The Raman spectra of uranophane, sklodowskite, cuprosklodowskite, boltwoodite and kasolite in the 700 to 1000 cm^{-1} region are shown in Figure 1. The infrared spectra of these minerals are displayed in Figure 2. The results of the spectroscopic analyses of the Raman and infrared spectra are reported in Tables 2 and 3 respectively. The Raman spectra show quite well-resolved bands in comparison with the infrared bands where a complex spectral profile with overlapping bands is observed.

The Raman spectra clearly show two clearly distinguishable spectral regions (a) in the 750 to 800 cm^{-1} region and (b) in the 950 to 1000 cm^{-1} region. The first region is assigned to the ν_1 mode of the $(UO_2)^{2+}$ units. The second region is attributed to the vibrations of the $(SiO_4)^{4-}$ tetrahedra. An intense band is observed at 796.9 cm^{-1} for uranophane; the band is sharp with a bandwidth of 16.9 cm^{-1}. Biwer et al. used a Raman microprobe to study some selected uranyl compounds including some uranyl silicates [17]. It was found that the most intense Raman band was observed between 738 and 842 cm^{-1} which was assigned to the symmetric stretching mode of the uranyl ion [17]. In the infrared spectra (Figure 2) the most intense band is observed at 832.7 cm^{-1} with a shoulder at 792.3 cm^{-1}. This latter band corresponds to the strong Raman band in this position and is assigned to the symmetric stretching mode of the $(UO_2)^{2+}$ units whilst the first band is assigned to the ν_3 antisymmetric stretching mode of the $(UO_2)^{2+}$ units. This band is not observed in the Raman spectrum of uranophane; however a very low intensity band is observed at around 888 cm^{-1}. Čejka reported in the infrared spectrum of a β-uranophane [16]. Čejka found a band at 854 cm^{-1}; although a second band is shown in the spectra (page 544) at around 880 cm^{-1} which appears to

correspond with the Raman band. Čejka reported the symmetric stretching mode at 777 cm^{-1} for β-uranophane [16].

For the mineral sklodowskite three Raman bands are found at 827.4, 800.9 and 777.0 cm^{-1} with bandwidths of 16.8, 13.4 and 15.9 cm^{-1}. The complexity of the infrared spectral profile makes the exact positioning of the bands difficult. This complexity for the minerals sklodowskite and cuprosklodowskite is also reflected in the infrared patterns reported by Čejka (page 536) [16]. Intense infrared bands are observed at 854.2, 820.6 and 787 cm^{-1} for sklodowskite. The width of these bands is when compared with that of the Raman spectra, quite broad (Table 3). One probable assignment of these bands is that the first two bands (827.4, 800.9) are due to the ν_3 antisymmetric stretching mode and the last band (777.0 cm^{-1}) to the ν_1 symmetric stretching mode. Čejka using infrared data reported these bands to be at 864 and 763 cm^{-1} which is in reasonable agreement with the band positions reported in this work [16]. Chernorukov et al. reported the infrared spectra of synthetic sklodowskite and gave the spectral data as (a) alpha polymorph: ν OH (H_2O) 3487; δ H_2O 1633; ν Si-OH 3300; δ SiOH 1373; ν_3 UO_2^{2+} 933; ν SiO_4 1167, 1080, 937, 860, 760, 680; δ SiO_4 600, 560, 500, 427 cm^{-1} and (b) beta polymorph: ν OH (H_2O) 3493; δ H_2O 1647, 1633; ν SiOH 3300; δ SiOH 1380; ν_3 UO_2^{2+} 940; ν SiO_4 1167, 1087, 1000, 860, 827, 760, 667; δ SiO_4 600, 557, 500, 453, 433 [24]. Because Chernorukov did not assign the individual bands, any comparison is difficult; however there is some correspondence of the Raman bands with Chernorukov's infrared data.

The Raman spectra of the cuprosklodowskite mineral shows much broader peaks with bands observed at 812.2 and 787 cm^{-1} with other low intensity bands

observed at 847.4 cm^{-1}, 774.4 and 758.8 cm^{-1}. Not only are considerable differences observed between sklodowskite and cuprosklodowskite in the Raman spectra but these differences are also observed in the infrared spectrum. Such differences were also observed in the infrared spectra of Čejka (See Figure page 536 of reference 16) [16]. Čejka reported the symmetric and antisymmetric stretching modes of cuprosklodowskite to be at 777 and 871 cm^{-1}. In these spectra however it is obvious other bands are present but not listed. To date no other Raman data is available for these minerals. Chernorukov et al. reported the infrared spectra of synthetic cuprosklodowskite and gave bands as ν_3 OH (H_2O) 3541.3; ν_1 H_2O 3412.8; δ H_2O 1645; ν SiOH 3353.6; δ SiOH 1380.6;; ν SiO_4 1094.1, 977.8, 865.2, 831.2; δ SiO_4 619.7, 576.6 cm^{-1} [50]. The band at ν_3 UO_2^{2+} 903.2 cm^{-1} is observable but is not mentioned in the text.

The Raman spectrum of boltwoodite shows complexity of the UO stretching vibrations of the $(UO_2)^{2+}$ units. Three bands are observed at 798.9, 796 and 785.6 cm^{-1}. The observation of three bands is probably due to the nonequivalence of the UO bonds. In the infrared spectrum of boltwoodite a strong reflectance band is found at 830 cm^{-1} with other bands at 782.6 and 761.8 cm^{-1}. Čejka from the infrared spectrum reported the symmetric stretching vibration at 787 cm^{-1}. He also gave the ν_3 vibration at 853 cm^{-1}. No bands were found in this position in this work in the Raman spectrum. Two low intensity bands were observed at 882.5 and 833.9 cm^{-1}. The first band may be assigned to the ν_3 antisymmetric stretching vibration. It is noteworthy that there have been several reports of the synthesis of boltwoodite and sodium boltwoodite [36,51]. Gevorkyan et al. reported the infrared spectrum of sodium boltwoodite and gave

ν_3 and ν_1 vibrational modes at 880 and 780 cm^{-1}. Some variation in band position is simply the result of cationic substitution. Chernorukov et al. have undertaken many studies of uranyl silicates, many of which have been synthesised and many of which have no natural equivalents [20-22]. Chernorukov et al. reported the infrared spectra of a synthetic analogue of boltwoodite [21]. Bands were listed as ν OH (H_2O) 3454; δ H_2O 1625; ν Si-OH 3182; δ 1360; ν_3 SiO_4 1100, 1060, 1000, 910, 836, 724; ν_4 SiO_4 640, 566, 484; ν_3 UO_2^{2+} 938, 883 cm^{-1}. In these papers of Chernorukov et al., the SiO_4 stretching and bending vibrations are given as ν SiO_4 and δ SiO_4, without any further separation of the ν_3 and ν_1 and δ_4 and δ_2 SiO_4. The infrared spectrum of a synthetic sodium boltwoodite was also given with data: ν OH (H_2O) 3511; δ H_2O 1637; ν SiO_4 1151, 1025, 978, 751, 685; δ SiO_4 625, 505, 471; ν_3 UO_2^{2+} 851 cm^{-1} [52]. The specific bands are not assigned and any comparison with the results of the Raman spectra reported in this work is difficult.

The Raman spectrum of kasolite shows an intense band at 758.7 cm^{-1}. The band is sharp with a bandwidth of 9.9 cm^{-1}. Other low intensity bands are found at 793.9 cm^{-1} with bandwidth of 16.5 cm^{-1}, 766.6 cm^{-1} with bandwidth of 23.2 cm^{-1} and 750 cm^{-1} with bandwidth of 21.3 cm^{-1}. In the infrared spectrum strong reflectance bands are observed at 820.3, 789.0 cm^{-1} with other less intense bands at 745 and 724.4 cm^{-1}. Čejka did not report the symmetric stretching mode for the $(UO_2)^{2+}$ unit for kasolite but did report the ν_3 mode at 904 cm^{-1}. One of the problems associated with the infrared spectra id the possible overlap between the bands assigned to the ν_3 modes of the $(UO_2)^{2+}$ units and the ν_1 mode of the SiO_4^{4-} units.

Chernorukov et al. reported the infrared spectra of a synthetic analogue of kasolite and gave infrared data as ν_3 OH (H_2O) 3443.1; δ H_2O 1598.1; ν_3 UO_2^{2+} 901.6; ν SiO_4 865.1, 840.7, 799.3; δ SiO_4 755.8, 569.0, 516.3, 459.7 cm^{-1}.

SiO_4^{4-} stretching vibrations

In the Raman spectrum of uranophane an intense band is observed at 960.5 cm^{-1}. This band is attributed to the ν_1 symmetric stretching mode of the SiO_4^{4-} units. A second band is observed at 963.9 cm^{-1} which is attributed to the same vibrational mode (Table 2). This work shows that there is no coincidence with the ν_3 mode of the $(UO_2)^{2+}$ unit. Čejka from the infrared spectrum of uranophane and β-uranophane reported the ν_3 modes of SiO_4^{4-} units at 942 and 1006 cm^{-1}. A low intensity band is observed in the Raman spectrum at 1005.2 cm^{-1} which may be ascribed to this band. In the infrared spectrum of uranophane three bands are observed at 1021.1, 989.3 and 931.8 cm^{-1}. These bands are separated from the set of bands attributed to the $(UO_2)^{2+}$ unit vibrations and may be assigned to the stretching vibrations of the SiO_4^{4-} units.

In the Raman spectrum of sklodowskite, three bands are observed at 970.2, 957.2 and 934.2 with bandwidths of 11.8, 19.5 and 13.5 cm^{-1} respectively. These bands are attributed to the ν_1 symmetric stretching mode of the SiO_4^{4-} units. A broad band was also observed at 1149.5 cm^{-1}. In the infrared spectrum of sklodowskite, four bands are observed at 1085.1, 1020.6, 979.6 and 926.5 cm^{-1}. These bands may be attributed to the ν_3 vibrations of the SiO_4^{4-} units. Čejka gave the ν_1 mode of the SiO_4^{4-} units as 850 cm^{-1} [16]. However in the light of the Raman data, this value does not appear to be correct. Čejka also gave the position of the ν_3 bands as 1163, 989 and 934 cm^{-1}[16]. The Raman spectrum of cuprosklodowskite shows an intense band at 974 cm^{-1} with a bandwidth of 15.7 cm^{-1} which is sharp. This band is assigned to the ν_1

mode of the SiO_4^{4-} units. In the infrared spectrum of cuprosklodowskite two strong bands are observed at 1075.9 and 979.6 cm^{-1}. These bands are attributed to the ν_3 vibrations of the SiO_4^{4-} units. Čejka reported these ν_3 modes of the SiO_4^{4-} units of cuprosklodowskite at 980 and 933 cm^{-1}. Chernorukov et al. gave infrared bands for a synthetic sklodowskite as ν SiO_4 1167, 1080, 937, 860, 760, 680; δ SiO_4 600, 560, 500, 427 cm^{-1}.

The Raman spectra of boltwoodite show bands of comparatively lesser intensity than the preceding minerals. Two bands are found at 958.2 and 936.1 cm^{-1} with bandwidths of 20.7 and 18.4 cm^{-1}. These bands are attributed to the ν_1 symmetric stretching mode of the SiO_4^{4-} units. In the infrared spectra intense reflectance bands are found at 1108.9, 1042.4, 993.4 and 930.5 cm^{-1}. The latter two bands may correspond to the Raman ν_1 modes. Čejka based upon infrared spectra suggested that the ν_1 symmetric stretching mode of the SiO_4^{4-} unit was at 875 cm^{-1} and that the ν_3 modes were at 987 and 935 cm^{-1}. In the light of the Raman data this assignment does not seem correct although Gevorkyan (1979) assigned two bands at 995 and 940 cm^{-1} to the ν_3 modes of the SiO_4^{4-} unit [51]. The three higher wavenumber bands in the infrared spectra (this work) are more likely to be the ν_3 antisymmetric stretching modes of the SiO_4^{4-} units. Chernorukov et al. gave bands for a synthetic analogue of boltwoodite as ν_3 SiO_4 1100, 1060, 1000, 910, 836, 724; ν_4 SiO_4 640, 566, 484 cm^{-1} [21]. No distinction was made between the symmetric and antisymmetric SiO_4 stretching modes. Chernorukov et al. gave bands for a synthetic sodium boltwoodite as ν SiO_4 1151, 1025, 978, 751, 685; δ SiO_4 625, 505, 471 cm^{-1} [52]. Any comparison with the data from the Raman spectra is difficult as the bands were not assigned.

In the Raman spectrum of kasolite an intense band is observed at 903.6 cm^{-1}. This band is attributed to the ν_1 symmetric stretching mode of the SiO_4^{4-} units. An alternative assignment would be to ν_3 UO_2^{2+} bands. However such an antisymmetric stretching band would not be as sharp or as intense in the Raman spectrum. In the infrared spectrum the most intense band is observed at 912 cm^{-1} with other bands of significant intensity at 1016.0, 971.0 and 890.7 cm^{-1}. The first band is the equivalent of the Raman band and the two higher wavenumber bands at 1016.0 and 971.0 cm^{-1} may be assigned to the ν_3 antisymmetric stretching mode of the SiO_4^{4-} units. Čejka based upon transmittance infrared spectra suggested two bands at 864 and 811 cm^{-1} were the ν_1 vibrational modes and the ν_3 mode was at 960 cm^{-1}. Chernorukov et al. gave bands for a synthetic kasolite as ν_3 OH (H_2O) 3443.1; δ H_2O 1598.1; ν_3 UO_2^{2+} 901.6; ν SiO_4 865.1, 840.7, 799.3; δ SiO_4 755.8, 569.0, 516.3, 459.7 cm^{-1}.

Uranyl bending vibrations

The Raman spectra of the low wavenumber region of the minerals studied in this work are shown in Figure 3. The results of the Raman spectroscopic analyses are reported in Table 2. One of the advantages of Raman spectroscopy is that bands below 500 cm^{-1} can be observed. The infrared ATR technique is limited by the lower wavenumber cut-off at around 550 cm^{-1}. For the mineral uranophane Raman bands of significant intensity are observed at 324.9, 288.9, 280.8, 250.3 and 213.7 cm^{-1}. Čejka based upon farIR spectra suggested that the ν_2 bending modes occurred at 286 or 316 or 280 cm^{-1}[153]. Thus it is possible that the three higher wavenumber bands belong to

the ν_2 bending mode. Čejka suggested that a possible coincidence of ν_2 δ $(UO_2)^{2+}$ and UO ligand vibrations [53]. The results of the Raman spectra lead to the conclusions that not only are the UO bond lengths different but that some of the $(UO_2)^{2+}$ units are not equivalent. Čejka suggested that a possible coincidence of ν_2 δ $(UO_2)^{2+}$ and UO ligand vibrations [53]. In the infrared and Raman spectra of $K_4(UO_2)(CO_3)_3$, Anderson et al. [54] ascribed bands in the range 241-307 cm^{-1} to the $(UO_2)^{2+}$ to the δ $(UO_2)^{2+}$ bending vibrations. It is possible that the two bands at 250.3 and 213.7 cm^{-1} are related to hydrogen bonding in the mineral. No reports of the doubly degenerate bending modes of the uranyl units of uranophane or β-uranophane have been reported.

In many ways the Raman spectra of the 100 to 300 cm^{-1} region of both sklodowskite and cuprosklodowskite are similar to that of uranophane. To the best of the authors' knowledge no data on the uranyl bending modes have been reported for this mineral. For sklodowskite, Raman bands are observed at 318.4, 304.6, 282.2, 264.0 and 217.3 cm^{-1}. The bands are quite sharp with bandwidths of 24.8, 14.2, 19.2, 13.8 and 21.8 cm^{-1}. For cuprosklodowskite, Raman bands are observed at 301.1, 276.7, 267.1, 217.7 and 205.8 cm^{-1}. The first two bands are attributed to ν_2 δ $(UO_2)^{2+}$. For boltwoodite Raman bands are observed at 314.0, 277.4 and 219.9 cm^{-1}. It is possible that the first two bands are due to the ν_2 bending modes of the $(UO_2)^{2+}$ units. In the only study that reports the bending modes of the uranyl unit, Plesko et al. based upon infrared data gave the position of the ν_2 $(UO_2)^{2+}$ bending mode as 280 cm^{-1} [118]. However a single band would negate the concept of the non-equivalence of the U-O bond lengths and this seems unlikely. In the Raman spectra of kasolite strong Raman bands are found at 302.5, 285.3, 234.3, 231.1 and 217.7 cm^{-1}.

SiO_4^{4-} bending vibrations

In the Raman spectra of uranophane, three bands are observed at 544.6, 469.5 and 398.9 cm^{-1}. The first band is assigned to the ν_4 bending mode of the SiO_4^{4-} units and the latter two bands to the ν_2 bending modes of the SiO_4^{4-} units. Čejka based upon infrared spectra reported two bands at 609 and 560 cm^{-1} and assigned these bands to the ν_4 bending mode of the SiO_4^{4-} units [16]. Čejka also found two bands at 485 and 460 cm^{-1} and assigned these bands to the ν_2 bending modes [16]. In the infrared spectra reported in this paper, the lower cut-off prevents the collection of data in this spectral region. The Raman spectra go a long way to identifying the bending modes of the SiO_4^{4-} units.

The Raman spectra of sklodowskite show four bands at 548.6, 473.8, 413.2 and 393.3 cm^{-1}. The first two bands are assigned to ν_4 bending modes of the SiO_4^{4-} units and the latter two modes to the ν_2 modes. Čejka reported a band at 570 cm^{-1} for sklodowskite and attributed this band to the ν_4 bending mode of the SiO_4^{4-} units [16]. He also reported two bands at 502 and 441 cm^{-1}. The band positions of the previous studies of Čejka differ from the Raman data reported in this work. The Raman spectra for cuprosklodowskite show strong resemblance to that of sklodowskite. Raman bands are observed at 535.1, 507.0, 476.8 and 411.2 cm^{-1}. The first two bands are assigned to the ν_4 SiO_4^{4-} bending modes and the latter two bands to the ν_2 SiO_4^{4-} bending modes. The Raman spectra in the 400 to 650 cm-1 region show no other bands making the assignment and attribution of the bands in this spectral region without difficulty.

The Raman spectra of boltwoodite display four bands at 537.3, 491.3, 464.8 and 397.2 cm^{-1}. The assignment of the bands is as above. Čejka provided data on boltwoodite and the two ν_4 modes were at 612 and 555 cm^{-1} and the two ν_2 modes at 486 and 448 cm^{-1}. In contrast Gevorkyan for a synthetic sodium boltwoodite gave ν_4 mode at 560 and 540 cm^{-1} and the ν_2 mode as 477 cm^{-1} [51]. The positions of the infrared bands do not correspond to the Raman band positions. For the mineral kasolite, Raman bands are observed at 575.9, 533.3, 501.1, 454.6 and 415.1 cm^{-1}. The first three bands may be attributed to the ν_4 SiO_4^{4-} bending modes and the latter two bands to the ν_2 SiO_4^{4-} bending modes. Čejka based upon the infrared spectra also showed three ν_4 bands at 563, 545 and 518 cm^{-1} [116]. These bands are in reasonable agreement with the Raman bands. The difference may be simply due to the methods of treating the data as explained above. No other spectroscopic information is available for these minerals.

OH stretching region

The Raman and infrared spectra of the hydroxyl stretching region are shown in Figures 4 and 5 respectively. The Raman and infrared spectra differ in that water is a much stronger absorber in the infrared spectrum than water is a Raman scatterer. Three intense bands are observed in the Raman spectrum of uranophane 3492.0, 3358.2 and 3215.6 cm^{-1}. The bands are very broad with bandwidths of 143.9, 131.9 and 151.2 cm^{-1}. In the infrared spectrum the most intense bands are found at 3407.1 and 3176.9 cm^{-1}. The bandwidths of these bands are very broad with widths of 225.6 and 343.9 cm^{-1}. The relatively low wavenumber positions for the water stretching

vibrations indicates strong hydrogen bonding in the mineral structure. The observation of more than one OH stretching vibration is indicative of the non-equivalence of the water molecules in the uranophane structure. Čejka reported OH stretching vibrations at 3437, 3200, 2920 and 2800 cm^{-1}[116]. For βuranophane two bands were reported at 3447 and 3225 cm^{-1}. In the spectra shown it is obvious other bands are present in the spectral profile but were not labelled. In uranophane there are two OH vibrating units (a) firstly the OH units of water and (b) the OH units from the SiO_3OH units. The position of SiOH bands is normally above 3600 cm^{-1}. Thus the bands observed above are all attributed to water OH stretching vibrations.

It is noted that Chernorukov et al. reported the SiOH stretching vibrations as 3200 cm^{-1} based upon the infrared spectra. However normally for zeolites and modified clay minerals, the SiOH stretching bands are found at wavenumbers > 3600 cm^{-1}. Often two SiOH bands are observed at 3730 and 3745 cm^{-1} which are assigned to hydrogen bonded and no-hydrogen bonded SiOH units. The band near 1400 cm^{-1} in silicates is connected with H(+) cation coordinated by O atoms, as it takes place in pectolite, babingtonite and other minerals [55-59]. In this case coordinating O atoms belong to polymerized silicate anion with two apical O at each Si. The H atom does not form strong covalent bonds with O. In silicates with isolated SiO_4, Si_2O_7 or Si_3O_{10} groups, Si with three apical O is present. In this case Si-O-H groups with essentially covalent O-H bonds can be formed (e. g. in rosenhahnite, afwillite etc.); acidic group Si-OH can have several states with different degree of charge separation between H and O. In IR spectra of such minerals a series of bands in the range 1300-3200 cm^{-1} can be present. However in some cases the acidic group Si-OH is not dissociated (as in some lovazerite-group minerals).

In uranophane and uranophane-beta neither dissociation, nor strong charge separation in the group O-H at Si takes place. The shoulder near 3200 cm^{-1} in the infrared spectra may correspond to this situation (in the case of uranophane-beta also the weak shoulder at 2200-2300 cm^{-1} is observed). However this seems unlikely. In other words the bands for the SiOH stretching vibrations are more likely to be at positions >3600 cm^{-1}.

In the Raman spectrum of sklodowskite three bands are observed at 3506.0, 3420.2 and 3316.4 cm^{-1}. In the infrared spectrum two low intensity bands are observed at 3688.9 and 3629.3 cm^{-1}. These bands are attributed to SiOH stretching vibrations. Intense bands are observed at 3511.7, 3282.0, 3042.9, 2924.7 and 2882.5 cm^{-1}. These bands may be ascribed to water stretching vibrations. Čejka reported bands for this mineral at 3490, 3317, 3200, 2900 and 2850 cm^{-1}[116]. For cuprosklodowskite Raman bands are observed at quite high wavenumbers at 3694.1 and 3571.1 cm^{-1}. It is possible that these are attributable to the SiOH stretching bands. Other Raman bands are found at 3499.3, 3435.2, 3282.0 and 2919.9 cm^{-1}. These bands are ascribed to water stretching vibrations. The number and position of these bands is indicative of strong hydrogen bonding of the water in the cuprosklodowskite structure. Also the multiplicity of the bands indicates the non-equivalence of these water units in the structure. These concepts are confirmed by the infrared spectra where infrared reflectance bands are observed at 3572.3, 3479.7, 3325.4, 3106.5 and 2914.8 cm^{-1}.

For the mineral boltwoodite, infrared bands are observed in the OH stretching region at 3527.1, 3402.6, 3278.5, 3080.6, 2912.4 cm^{-1}. Raman bands are found at

3576.2, 3510.2, 3434.5, 3206.2 and 2880.9 cm^{-1}. Čejka reported broad maxima for this mineral at 3386 and 3150 cm^{-1} [16]. On studying the published spectra other component bands are readily observed. Plesko et al. reported bands at 3465, 3390 and 3190 cm^{-1} [18]. Vochten et al. offered bands at 3469, 3401 and 3246 cm^{-1} [60]. Gevorkyan for a synthetic sodium boltwoodite gave bands at 3580, 3475 and 3410 cm^{-1} [51]. It is obvious that there is considerable variation in band position and the number of bands for this mineral.

The Raman spectrum of kasolite shows three intense bands at 3484.2, 3438.2, 3411.1 cm^{-1} with an additional low intensity band at 3166.4 cm^{-1}. The infrared spectrum showed intense bands at 3439.9, 3391.6 and 3176.7 cm^{-1} with other low intensity bands at 3516.1 and 2897.9 cm^{-1}. Čejka reported bands at 3421, 2923 and 2850 cm^{-1} for kasolite [16].

Water and SiOH bending modes

The infrared spectra of the minerals studied in this research in the 1400 to 1800 cm^{-1} range are shown in Figure 6. This region is where the water δ HOH bending modes are found. Further it is likely that additional bands in this spectral region can be assigned to δSiOH deformation modes. The infrared spectra of uranophane shows clearly resolved bands at 1664.5 and 1624.3 cm^{-1} assigned to the water bending modes as well as bands at 1557.9 and 1419.5 cm^{-1}. These bands are attributed to the δSiOH modes. Čejka reported δH_2O at 1636 cm^{-1} and δSiOH at 1541 cm^{-1}. This latter band agrees well with the infrared band reported above. Čejka also

reported two infrared bands for βuranophane at 1665 and 1636 cm^{-1}. These bands appear to correspond well with the position of the two δH_2O bands above.

For the mineral sklodowskite an intense band is observed in the infrared spectrum at 1643 cm^{-1} with two broad bands at 1548 and 1441.9 cm^{-1}. The first band is assigned to the δH2O mode and is at higher wavenumbers than is expected for hydrogen bonded water, indicating the water in sklodowskite is strongly hydrogen bonded. The latter two bands correspond to δSiOH modes. Čejka reported δSiOH bands at 1450 and 1410 cm^{-1} [16]. For cuprosklodowskite, infrared bands in this spectral region are observed in similar positions to those of sklodowskite found at 1611.4, 1536.4 and 1434.1 cm^{-1}. A band at 1450 cm^{-1} observed by Akhmanova was assigned to the δSiOH vibration [31].

The infrared spectrum of boltwoodite shows two resolved bands at 1682.5 and 1619.4 cm^{-1}. These bands are assigned to the δH_2O bands. The position of the first band is indicative of strong hydrogen bonding of the water molecules in the boltwoodite structure. The observation of two bands in this region indicates the non-equivalence of the water molecules in the structure. Two broad bands are observed at 1535.0 and 1453.0 cm^{-1}. These bands are assigned to the δSiOH vibrations.

Conclusions

Raman spectroscopy has enabled the characteristic spectra of a suite of uranyl silicates of the uranophane group to be obtained. These spectra are characteristic of the particular mineral being studied. The application of Raman spectroscopy enabled

excellent band separation with no overlap of bands due to different vibrating units as is found with infrared spectroscopy. This separation enabled definitive assignment of the bands.

Acknowledgements

The financial and infra-structure support of the Queensland University of Technology Inorganic Materials Research Program of the School of Physical and Chemical Sciences is gratefully acknowledged. The Australian Research Council (ARC) is thanked for funding.

Mr Dermot A. Henry of Museum Victoria is thanked for the supply of the uranyl silicate minerals.

References

1. Burns, PC. *Canadian Mineralogist* 2001**; 39**: 1153.
2. Jackson, JM, Burns, PC. *Canadian Mineralogist* 2001**; 39**: 187.
3. Burns, PC. *Canadian Mineralogist* 1998**; 36**: 1069.
4. Burns, PC, Miller, ML, Ewing, RC. *Canadian Mineralogist* 1996**; 34**: 845.
5. Burns, PC, Ewing, RC, Hawthorne, FC. *Canadian Mineralogist* 1997**; 35**: 1551.
6. Burns, PC. *Reviews in Mineralogy* 1999**; 38**: 23.
7. Burns, PC, Deely, KM, Skanthakumar, S. *Radiochimica Acta* 2004**; 92**: 151.
8. Burns, PC, Finch, R, Editors *Uranium: Mineralogy, Geochemistry and the Environment. (Proceedings of a Short Course held 22-23 October 1999 in Golden, Colorado.) [In: Rev. Mineral., 1999; 38]*, 1999.
9. Demartin, F, Gramaccioli, CM, Pilati, T. *Acta Crystallographica, Section C: Crystal Structure Communications* 1992**; C48**: 1.
10. Blaton, N, Vochten, R, Peeters, OM, Van Springel, K. *Neues Jahrbuch fuer Mineralogie, Monatshefte* 1999: 253.
11. Atencio, D, Carvalho, FMS, Matioli, PA. *American Mineralogist* 2004**; 89**: 721.
12. Sidorenko, GA, Moroz, IK, Zhil'tsova, IG. *Zapiski Vsesoyuznogo Mineralogicheskogo Obshchestva* 1975**; 104**: 559.
13. Sidorenko, GA, Chukanov, NV, Naumova, IS. *Mineralogicheskii Zhurnal* 2001**; 23**: 55.
14. Burns, PC, Hill, FC. *Canadian Mineralogist* 2000**; 38**: 163.
15. Huang, J, Wang, X, Jacobson, AJ. *Journal of Materials Chemistry* 2003**; 13**: 191.
16. Cejka, J. *Reviews in Mineralogy* 1999**; 38**: 521.
17. Biwer, BM, Ebert, WL, Bates, JK. *Journal of Nuclear Materials* 1990**; 175**: 188.
18. Plesko, EP, Scheetz, BE, White, WB. *American Mineralogist* 1992**; 77**: 431.
19. Li, Y, Cahill, CL, Burns, PC. *Chemistry of Materials* 2001**; 13**: 4026.
20. Chernorukov, NG, Kortikov, VE. *Zhurnal Neorganicheskoi Khimii* 2000**; 45**: 1949.
21. Chernorukov, NG, Kortikov, VE. *Radiochemistry (Moscow)(Translation of Radiokhimiya)* 2000**; 42**: 446.
22. Chernorukov, NG, Kortikov, VE. *Zhurnal Neorganicheskoi Khimii* 2000**; 45**: 1110.
23. Karyakin, NV, Chernorukov, NG, Suleimanov, EV, Trostin, VL, Alimzhanov, MI, Makarov, AV. *Russian Journal of General Chemistry (Translation of Zhurnal Obshchei Khimii)* 2001**; 71**: 1513.
24. Chernorukov, NG, Kortikov, VE. *Zhurnal Neorganicheskoi Khimii* 2001**; 46**: 1949.
25. Karyakin, NV, Chernorukov, NG, Suleimanov, EV, Trostin, VL, Alimzhanov, MI, Makarov, AV. *Zhurnal Fizicheskoi Khimii* 2001**; 75**: 1190.
26. Chernorukov, NG, Suleimanov, EV, Nipruk, OV. *Russian Journal of General Chemistry (Translation of Zhurnal Obshchei Khimii)* 2001**; 71**: 1001.
27. Chernorukov, NG, Kortikov, VE. *Radiochemistry (Moscow, Russian Federation)(Translation of Radiokhimiya)* 2002**; 44**: 446.

28. Chernorukov, NG, Kortikov, VE. *Zhurnal Neorganicheskoi Khimii* 2002**; 47**: 232.
29. Burns, PC, Deely, KM. *Canadian Mineralogist* 2002**; 40**: 1579.
30. Burns, PC. *Materials Research Society Symposium Proceedings* 2004**; 802**: 89.
31. Akhmanova, MV, V.Karyakin, A, Yukhnevich, GB. *Geokhimiya* 1963**; 6**: 581.
32. Plyusnina, II *Infrared Spectra of Minerals*, 1977.
33. Gevork'yan, SV, Povarennykh, AS. *Mineralogicheskii Zhurnal* 1980**; 2**: 29.
34. Gevork'yan, SV, Povarennykh, AS, Ignatov, SI, Il'chenko, EA. *Mineralogicheskii Zhurnal* 1981**; 3**: 3.
35. Cejka, J, Urbanec, Z. *Transactions of the Czechoslovak Academy of Sciences, Math. Natur. History Series, Academia Prague.* 1990**; 100**: 1.
36. Vochten, R, Blaton, N, Peeters, O. *Neues Jahrbuch fuer Mineralogie, Monatshefte* 1997: 569.
37. Nyfeler, D, Armbruster, T. *American Mineralogist* 1998**; 83**: 119.
38. Frost Ray, L. *Spectrochimica acta. Part A, Molecular and biomolecular spectroscopy* 2004**; 60**: 1469.
39. Frost Ray, L, Weier, M. *Spectrochimica acta. Part A, Molecular and biomolecular spectroscopy* 2004**; 60**: 2399.
40. Frost, RL. *Spectrochimica Acta, Part A: Molecular and Biomolecular Spectroscopy* 2004**; 60A**: 1469.
41. Frost, RL, Carmody, O, Erickson, KL, Weier, ML, Cejka, J. *Journal of Molecular Structure* 2004**; 703**: 47.
42. Frost, RL, Henry, DA, Erickson, K. *Journal of Raman Spectroscopy* 2004**; 35**: 255.
43. Frost, RL, Weier, ML. *Journal of Raman Spectroscopy* 2004**; 35**: 299.
44. Frost, RL, Weier, ML, Adebajo, MO. *Thermochimica Acta* 2004**; 419**: 119.
45. Nakamoto, K. *J. Wiley & Sons, New York, 484 pp.* 1986.
46. McMillan, P. *American Mineralogist* 1984**; 69**: 622.
47. Huang, Y, Jiang, Z, Schwieger, W. *Canadian Journal of Chemistry* 1999**; 77**: 495.
48. Huang, Y, Jiang, Z, Schwieger, W. *Chemistry of Materials* 1999**; 11**: 1210.
49. Andreev, GB, Fedoseev, AM, Perminov, VP, Budantseva, NA. *Radiochemistry (Moscow, Russian Federation)(Translation of Radiokhimiya)* 2003**; 45**: 488.
50. Chernorukov, NG, Knyazev, AV, Sergacheva, IV. *Zhurnal Neorganicheskoi Khimii* 2003**; 48**: 213.
51. Gevork'yan, SV, Matkovskii, AO, Povarennykh, AS, Sidorenko, GA. *Mineralogicheskii Zhurnal* 1979**; 1**: 78.
52. Chernorukov, NG, Kortikov, VE. *Radiochemistry (Moscow, Russian Federation)(Translation of Radiokhimiya)* 2001**; 43**: 229.
53. Cejka, J. *Reviews in mineralogy* 1999**; 38**.
54. Anderson, A, Chieh, C, Irish, DE, Tong, JPK. *Canadian Journal of Chemistry* 1980**; 58**: 1651.
55. Beran, A, Libowitzky, E. *NATO Science Series, Series C: Mathematical and Physical Sciences* 1999**; 543**: 493.
56. Henning, O, Gerstner, B. *Wissenschaftliche Zeitschrift der Hochschule fuer Architektur und Bauwesen Weimar* 1972**; 19**: 287.

57. Kroenert, W, Siegert, M. *Tonindustrie-Zeitung und Keramische Rundschau* 1974**; 98**: 188.
58. Kroenert, W, Siegert, M. *Tonindustrie-Zeitung und Keramische Rundschau* 1975**; 99**: 9.
59. Ryskin, YI, Stavitskaya, GP, Toropov, NA. *Zhurnal Neorganicheskoi Khimii* 1960**; 5**: 2727.
60. Vochten, R, Blaton, N, Peeters, O, Van Springel, K, Van Haverbeke, L. *Canadian Mineralogist* 1997**; 35**: 735.

Appendix: Curve resolution.

The protocol for band fitting the spectra is as follows:

(a) The spectra are collected with the highest signal to noise ratio within a reasonable time frame.
(b) The spectra are converted to a spc file using Grams ® software.
(c) This software is then used to baseline correct the spectra using a multipoint fitting function.
(d) The spectrum is then converted to an ascii type form (.prn) for reading into the Jandel 'peakfit' ® software program.
(e) The spectra are then fitted with the minimum number of bands required to fit the experimental profile with the sum of the component bands. The number of bands used is chosen so that the residual is of the same dimension as the noise.
(f) The difference between these is then checked.
(g) Normally the sum of the component bands is plotted over the experimental profile to show that there is no difference.
(h) The reiterations of the band fitting are undertaken until an r^2 value of > 0.9995 is obtained. This is essentially ensuring that the deviation between the experimental and theoretical profiles approaches zero. The signal to noise determines the value of r^2 that can be achieved.
(i) The type of function used in the fitting process is a Gauss-Lorentzian cross-product function. Previous research by the author found that this was the most suitable function for fitting Raman spectral profiles.
(j) It is probably true that this is not the best function for fitting infrared bands which may contain hot bands but it is certainly the most useful for fitting Raman bands.
(k) The whole Raman spectra are fitted and the fitted spectra are then sectioned into relevant spectral regions for presentation.
(l) Justification of the number of bands and the position of the bands is made in terms of the chemistry of the particular mineral and its structure.

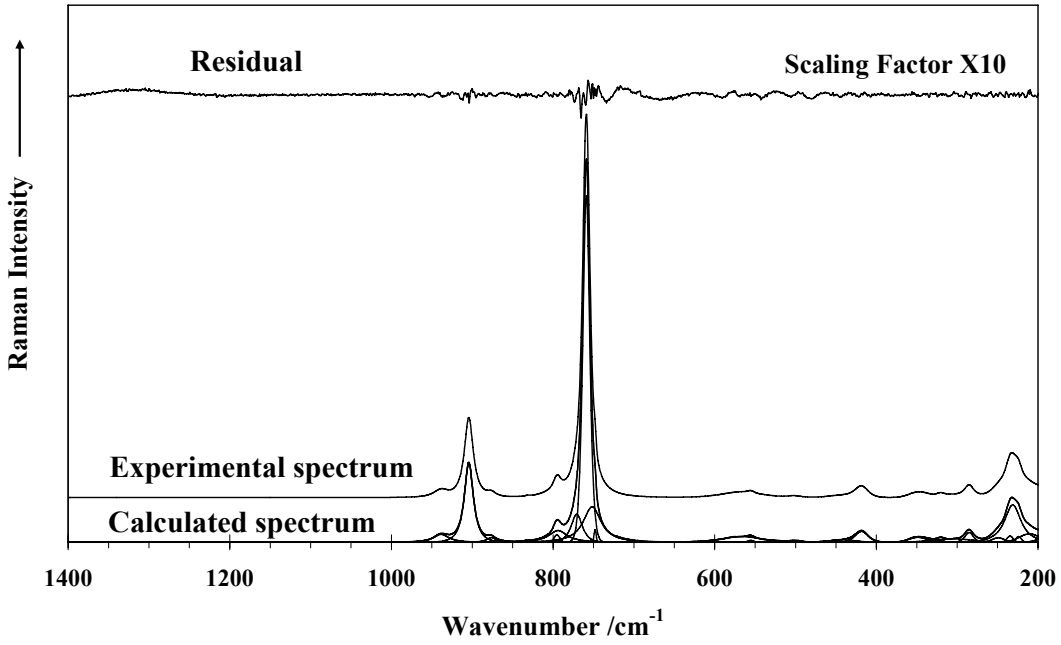

The above figure shows the Raman spectrum of kasolite (sample M33152). The figure shows the residual band scaled X 10 which is the difference between the experimentally determined band profile and the calculated band profile. The calculated spectrum is identical to the experimental spectrum.

It should also be noted that the reason for obtaining spectra at 77 K are to confirm the band positions and the number of bands in the spectrum at 298 K.

Ray Frost

Table 1 Sample details

Mineral	**Formula**	**Locale**	#
Uranophane	$Ca(UO_2)_2(SiO_3OH)_2 \cdot 5H_2O$	Shaba, Congo, Zaire	M31300
Sklodowskite	$Mg(UO_2)_2(SiO_3OH)_2 \cdot 5H_2O$	Eva Mine, Northern Territory	M37839
Cuprosklodowskite	$Cu(UO_2)_2(SiO_3OH)_2 \cdot 6H_2O$	Shinkolobwe mine, Shaba Province, Congo, Zaire	M33423
Boltwoodite	$(K,Na)[(UO_2)(SiO_3OH)] \cdot 1.5H_2O$	Arandis, Namibia	M30851
Kasolite	$PbUO_2SiO_4 \cdot H_2O$	El Sharana mine, South Alligator River, Northern Territory	M33152

Table 2 Raman spectral analysis of the uranyl silicates

uranophane			**sklodowskite**			**cupro sklodowskite**			**boltwoodite**			**kasolite**		
m31300			m37839			m33423			m30851			m33152		
Centre	FWHM	%	**Centre**	FWHM	%	**Centre**	FWHM	%	**Centre**	FWHM	%	**Centre**	FWHM	%
						3694.1	30.8	0.2						
						3571.1	40.8	0.6	**3576.2**	56.1	2.7			
			3506.0	107.3	47.8				**3510.2**	87.7	2.8			
3492.0	143.9	28.1				**3499.3**	107.6	4.8				**3484.2**	102.4	25.0
3462.6	31.6	0.7												
						3435.2	219.8	39.9	**3434.5**	268.9	25.8	**3438.2**	57.7	49.2
			3420.2	83.1	15.1							**3411.1**	224.1	24.6
3358.2	131.9	47.7												
			3316.4	145.8	37.1									
						3282.0	369.1	43.6						
3215.6	151.2	9.1							**3206.2**	384.7	67.2			
												3166.4	107.7	1.3
						2919.9	350.4	10.9						
2899.7	124.2	5.9							**2880.9**	132.0	1.4			
2728.6	135.0	5.3												
2476.8	92.8	2.3												
2136.8	98.1	1.0												
			1640.0	111.7	2.2									
									1597.5	67.0	0.9	**1593.7**	61.4	0.6
			1528.4	155.1	10.0									
						1503.6	242.9	17.4						
			1413.4	140.7	10.3									
			1311.8	111.3	4.1				**1316.0**	109.7	1.5			
						1296.8	238.9	11.2						
			1243.5	75.8	7.9	**1246.3**	67.7	2.3						

			1149.5	78.3	4.9	**1156.2**	71.9	3.6						
1005.2	23.4	0.1							**1008.5**	7.0	0.1			
			986.0	33.7	0.9									
963.9	10.2	2.9	**970.2**	11.8	6.2	**974.0**	15.7	4.9						
960.5	25.7	14.7	**957.2**	19.5	1.6				**958.2**	20.7	7.7			
950.2	10.1	0.4												
			934.2	13.5	2.5				**936.1**	18.4	4.6	**939.9**	15.9	2.5
						919.2	17.4	0.4						
						916.6	50.7	2.3						
			896.9	10.3	0.1	**901.1**	11.2	0.3				**903.6**	14.5	4.7
885.6	19.4	1.3							**882.5**	16.2	0.3	**886.3**	5.9	0.4
												876.2	14.6	1.2
			852.8	12.2	0.1	**847.4**	61.9	0.9						
839.0	14.6	0.3							**833.9**	29.7	4.9			
			827.4	16.8	1.4							**820.8**	28.5	0.5
						812.2	15.2	2.9						
796.9	16.9	27.8	**800.9**	13.4	6.1				**798.9**	13.8	34.7	**793.9**	16.5	4.2
792.9	63.2	19.8							**796.0**	13.3	9.3			
786.4	29.0	3.3				**787.0**	47.0	27.6	**785.6**	21.5	14.3			
			777.0	15.9	22.5	**774.4**	13.2	0.6				**766.7**	23.2	10.0
			754.8	33.3	0.9	**758.8**	11.5	0.7				**758.7**	9.9	35.4
						746.7	68.9	1.8	**744.5**	85.4	2.4	**750.0**	21.3	10.0
711.4	87.8	2.5										**721.3**	49.1	1.6
												575.9	38.3	2.3
544.6	14.6	2.0	**548.6**	26.0	1.6							**550.4**	14.0	0.4
						535.1	20.7	1.4	**537.3**	15.8	2.2	**533.3**	38.3	0.8
						507.0	50.3	0.3				**501.1**	17.2	0.6
									491.3	24.9	0.8			
469.5	20.8	1.2	**473.8**	32.4	1.2	**476.8**	21.8	0.3						
									464.8	20.9	0.8	**454.6**	26.9	0.3
			413.5	22.2	2.3	**411.2**	30.5	0.5				**415.1**	21.6	1.1
398.9	26.3	3.9	**393.3**	24.2	0.6				**397.2**	24.7	2.1			

376.5	7.0	0.1				**386.9**	22.8	4.1	**375.7**	17.1	0.3			
347.3	9.7	0.1										**341.4**	22.2	0.7
324.9	24.9	3.2	**318.4**	24.8	1.6				**321.8**	8.7	0.2	**319.0**	13.5	2.8
									314.0	21.3	3.0			
306.5	15.1	0.7	**304.6**	14.2	1.1	**301.1**	15.1	5.0				**302.5**	16.4	1.2
288.9	34.4	7.1	**282.2**	19.2	2.6				**293.5**	9.7	0.1	**285.3**	16.2	3.2
280.5	20.6	2.0				**276.7**	13.5	2.9	**277.4**	17.5	1.6			
			264.0	13.8	1.3	**267.1**	28.2	2.3	**263.1**	16.4	0.4			
250.3	19.8	2.0										**234.3**	10.3	1.2
												231.1	14.2	2.2
213.7	31.0	2.0	**217.3**	21.8	1.1	**217.7**	47.5	2.5	**219.9**	25.3	6.0	**217.7**	55.6	6.6
									215.1	7.7	0.2			
205.2	9.7	0.4				**205.8**	17.2	1.2						
			199.9	15.3	1.0									
			196.7	35.6	1.4	**184.5**	20.8	1.7				**184.7**	14.8	1.6
166.7	14.1	0.9				**164.8**	15.5	0.8	**166.1**	9.1	0.1	**165.3**	14.4	2.4
			155.9	33.3	1.9							**153.5**	16.3	0.6
139.5	27.8	0.3	**137.2**	10.5	0.2				**140.1**	21.5	1.2	**140.1**	8.8	0.3
137.4	13.7	0.5				**133.9**	6.6	0.0						
122.1	9.2	0.2	**127.3**	17.9	0.3									
112.4	9.0	0.2	**112.7**	8.3	0.2	**113.6**	10.8	0.2	**117.6**	15.4	0.4	**107.5**	13.8	0.6
												99.6	8.6	0.0

Table 3 Infrared spectral analysis of selected uranyl silicates

uranophane			sklodowskite			cupro sklodowskite			boltwoodite			kasolite		
	m31300			m37839			m33423			m30851			m33152	
Centre	FWHM	%	**Centre**	FWHM	%	**Centre**	FWHM	%	**Centre**	FWHM	%	**Centre**	FWHM	%
			3688.9	32.6	0.6							**3694.3**	26.6	0.1
			3629.3	58.6	0.8							**3616.9**	48.6	0.3
						3572.3	56.8	0.8						
3546.4	102.0	1.9												
			3511.7	160.0	6.2				**3527.1**	113.9	3.1	**3516.1**	48.1	1.0
						3479.7	155.0	3.2	**3471.2**	43.9	0.4			
												3439.9	77.2	3.6
3407.1	225.6	17.6							**3402.6**	89.2	5.3	**3391.6**	214.2	11.8
						3325.4	254.0	13.5	**3329.9**	55.7	0.4			
			3282.0	372.3	24.6				**3278.5**	248.9	13.9			
3176.9	343.9	22.5										**3176.7**	358.3	14.4
						3106.5	284.3	16.0	**3080.6**	247.3	11.4			
			3042.9	283.5	7.1									
2920.4	20.3	0.0	**2924.7**	39.6	0.5	**2914.8**	181.8	4.7	**2912.4**	187.3	2.6			
2918.4	119.7	0.6												
			2882.5	255.0	4.0							**2897.9**	185.9	1.5
2867.4	345.2	8.0												
2849.3	27.5	0.0												
						2791.8	146.6	2.0						
									2746.0	207.8	1.2			
						2705.0	91.2	0.5						
1664.5	44.2	1.2							**1682.5**	18.6	0.6			
			1643.0	72.7	4.0									
1624.3	50.7	2.4							**1625.4**	86.5	2.7			
						1611.4	76.1	3.6	**1619.4**	14.2	0.5			
												1595.2	19.0	0.8

									1574.4	71.8	2.4
1557.9	150.9	2.0	**1548.2**	73.8	0.5						
1530.2	32.9	0.1				**1536.4**	86.3	1.1			
									1475.5	215.2	2.7
			1441.9	101.6	0.8	**1434.1**	61.4	0.7			
1419.5	113.2	1.4									
1322.6	36.1	0.1							**1311.1**	38.1	0.1
1283.7	33.8	0.1									
1144.7	44.0	0.7	**1159.1**	33.2	1.0				**1137.8**	5.9	0.0
1115.1	15.8	0.0	**1122.8**	37.9	0.8				**1108.9**	80.9	9.6
1099.7	17.2	0.1	**1085.1**	43.9	1.5						
						1075.9	57.8	1.4			
									1042.4	50.7	1.4
1021.1	43.3	2.1	**1020.6**	60.7	7.3						
989.3	38.2	4.1				**997.6**	101.8	8.0	**993.4**	64.7	4.8
			979.6	43.9	7.4	**979.2**	32.7	1.0	**977.9**	22.7	0.6
931.8	48.3	4.7	**926.5**	48.3	7.4				**930.5**	41.7	5.3
915.2	24.7	0.6				**911.3**	58.7	8.2	**915.3**	22.8	1.1
									873.0	47.5	6.8
			854.2	72.5	17.3	**856.7**	45.5	9.2			
832.7	75.5	19.8									
827.0	22.8	0.7	**820.6**	40.7	2.2	**822.1**	60.9	11.4	**830.0**	51.3	16.4
792.3	23.9	0.8	**787.1**	22.3	0.7				**782.6**	30.0	3.5
						771.5	15.6	0.3			
766.9	37.5	3.6				**767.0**	67.9	3.1	**761.8**	78.2	5.3
740.2	60.1	3.1	**756.9**	54.9	1.9						
						713.4	152.2	9.2			
			687.9	39.5	1.0						
653.2	47.6	0.7							**666.2**	20.0	0.9
									599.6	15.8	0.6

1016.0	45.6	1.5
971.0	53.0	4.6
912.0	65.4	11.8
890.7	30.8	6.4
866.9	7.4	0.4
860.0	11.6	1.2
848.4	9.7	0.4
839.4	8.8	0.3
820.3	40.0	7.7
789.0	40.2	9.8
745.0	30.8	2.4
724.4	86.0	9.0
658.8	61.2	2.1

			566.4	22.4	0.2	**575.0**	43.6	0.4				**562.5**	18.5	0.9
550.9	28.6	1.1	**540.1**	60.3	2.1	**551.9**	27.2	1.8	**552.7**	28.1	1.8	**544.9**	20.7	2.6

List of Figures

Figure 1 Raman spectra of uranophane, sklodowskite, cuprosklodowskite, boltwoodite and kasolite in the 700 to 1000 cm^{-1} region.

Figure 2 Infrared ATR spectra of uranophane, sklodowskite, cuprosklodowskite, boltwoodite and kasolite in the 5500 to 1200 cm^{-1} region.

Figure 3 Raman spectra of uranophane, sklodowskite, cuprosklodowskite, boltwoodite and kasolite in the 100 to 650 cm^{-1} region.

Figure 4 Raman spectra of uranophane, sklodowskite, cuprosklodowskite, boltwoodite and kasolite in the 2600 to 3800 cm^{-1} region.

Figure 5 Infrared ATR spectra of uranophane, sklodowskite, cuprosklodowskite, boltwoodite and kasolite in the 2500 to 3750 cm^{-1} region.

Figure 6 Infrared ATR spectra of uranophane, sklodowskite, cuprosklodowskite, boltwoodite and kasolite in the 1300 to 1800 cm^{-1} region.

List of Tables

Table 1 Minerals, their formulation and their origin

Table 2 Raman spectral analysis of the uranyl silicates

Table 3 Infrared spectral analysis of selected uranyl silicates

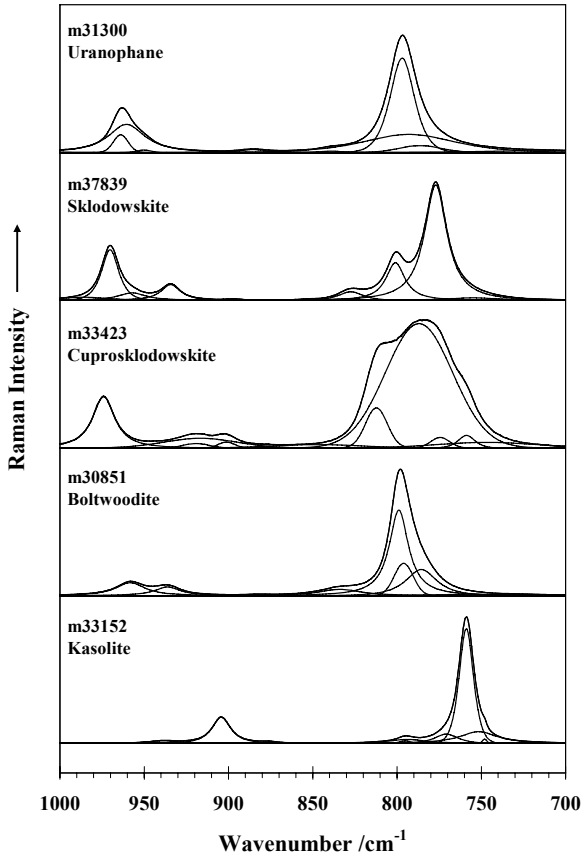
m31300
Uranophane
m37839
Sklodowskite
m33423
Cuprosklodowskite
m30851
Boltwoodite
m33152
Kasolite
Raman Intensity
1000
950
900
850
800
750
700
Wavenumber /cm-1

Figure 1

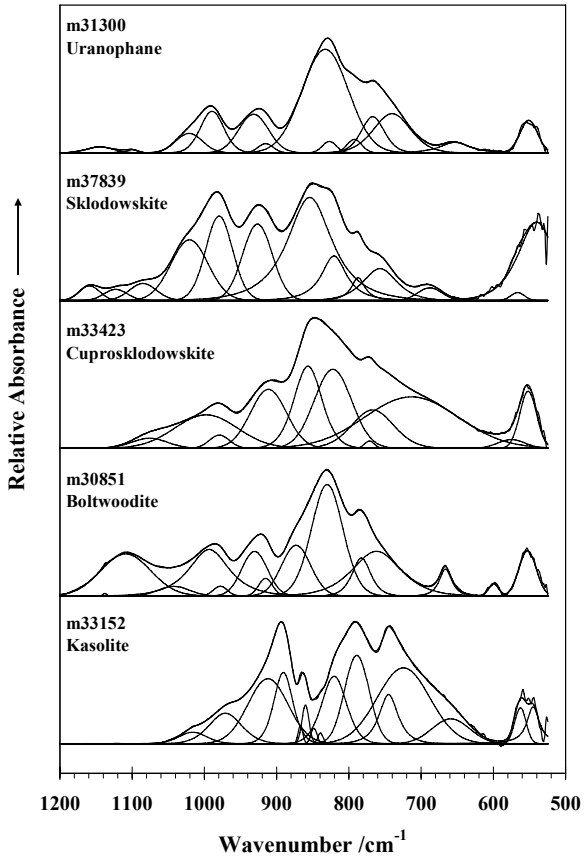

Figure 2 Infrared

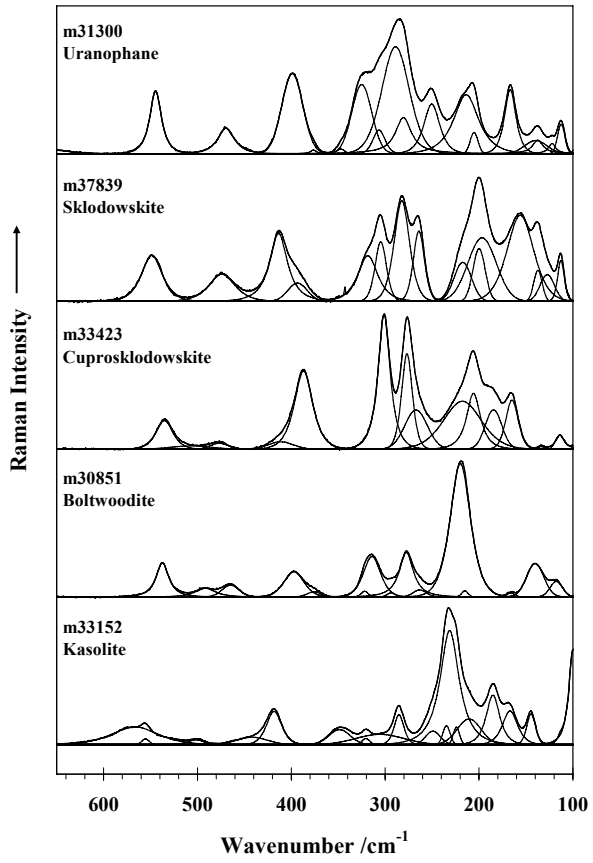
m31300
Uranophane
m37839
Sklodowskite
m33423
Cuprosklodowskite
m30851
Boltwoodite
m33152
Kasolite
Raman Intensity
600
500
400
300
200
100
Wavenumber /cm-1

Figure 3

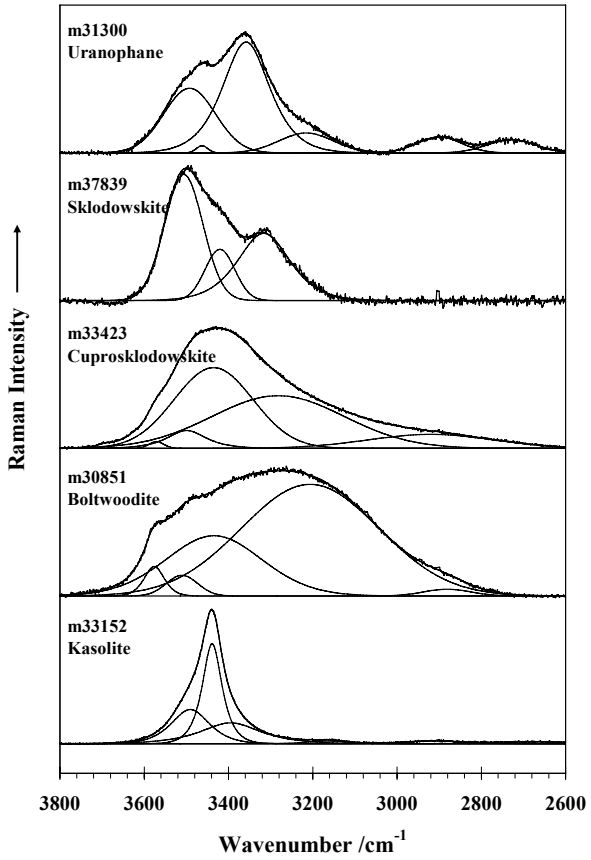
m31300
Uranophane
m37839
Sklodowskite
m33423
Cuprosklodowskite
m30851
Boltwoodite
m33152
Kasolite
Raman Intensity
3800
3600
3400
3200
3000
2800
2600
Wavenumber /cm-1

Figure 4

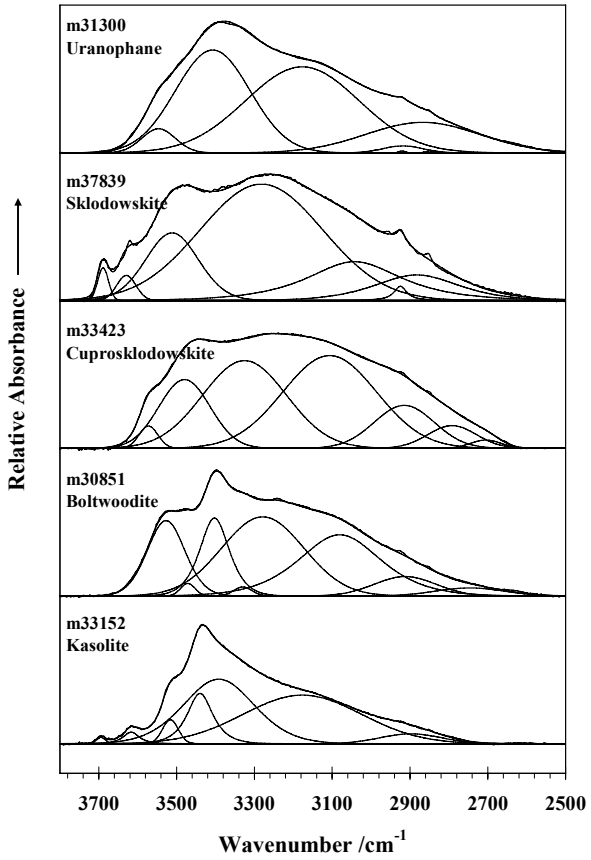
m31300
Uranophane
m37839
Sklodowskite
m33423
Cuprosklodowskite
m30851
Boltwoodite
m33152
Kasolite
Relative Absorbance
3700
3500
3300
3100
2900
2700
2500
Wavenumber /cm-1

Figure 5

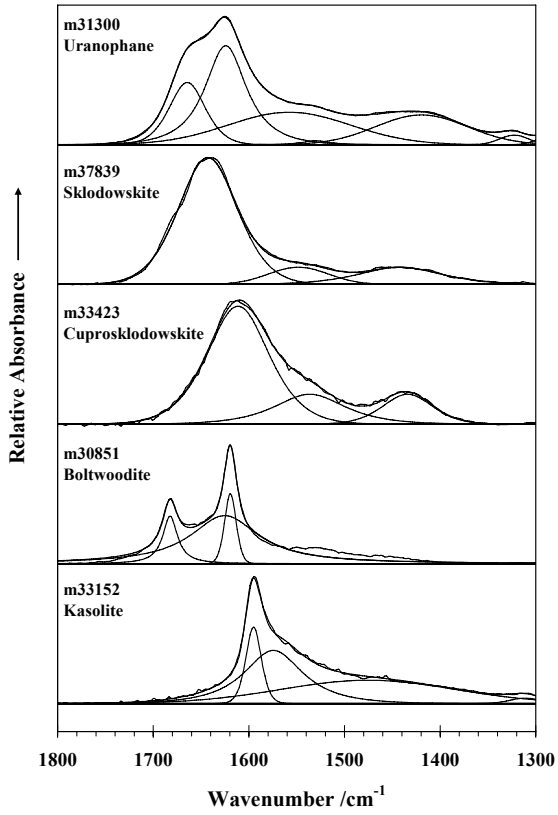
m31300
Uranophane
m37839
Sklodowskite
m33423
Cuprosklodowskite
m30851
Boltwoodite
m33152
Kasolite
Relative Absorbance
1800
1700
1600
1500
1400
1300
Wavenumber /cm-1

Figure 6